

## NEW EVIDENCE FOR THE DYNAMICAL DECAY OF A MULTIPLE SYSTEM IN THE ORION KLEINMANN-LOW NEBULA<sup>1</sup>

K. L. LUHMAN<sup>2,3</sup>, M. ROBERTO<sup>4,5</sup>, J. C. TAN<sup>6,7</sup>, M. ANDERSEN<sup>8</sup>, M. GIULIA UBEIRA GABELLINI<sup>4,9</sup>, C. F. MANARA<sup>10</sup>, I. PLATAIS<sup>11</sup>, & L. UBEDA<sup>4</sup>

*Draft version March 26, 2018*

### ABSTRACT

We have measured astrometry for members of the Orion Nebula Cluster with images obtained in 2015 with the Wide Field Camera 3 on board the *Hubble Space Telescope*. By comparing those data to previous measurements with NICMOS on *Hubble* in 1998, we have discovered that a star in the Kleinmann-Low Nebula, source x from Lonsdale et al. (1982), is moving with an unusually high proper motion of 29 mas yr<sup>-1</sup>, which corresponds to 55 km s<sup>-1</sup> at the distance of Orion. Previous radio observations have found that three other stars in the Kleinmann-Low Nebula (BN and sources I and n) have high proper motions (5–14 mas yr<sup>-1</sup>) and were near a single location ~540 years ago, and thus may have been members of a multiple system that dynamically decayed. The proper motion of source x is consistent with ejection from that same location 540 years ago, which provides strong evidence that the dynamical decay did occur and that the runaway star BN originated in the Kleinmann-Low Nebula rather than the nearby Trapezium cluster. However, our constraint on the motion of source n is significantly smaller than the most recent radio measurement, which indicates that it did not participate in the event that ejected the other three stars.

*Subject headings:* astrometry — stars: formation — stars: kinematics and dynamics — stars: pre-main sequence — stars: protostars

### 1. INTRODUCTION

The Kleinmann-Low (KL) Nebula is a source of extended infrared (IR) emission that is located 1' northwest of the Trapezium stars in the Orion Nebula Cluster (Kleinmann & Low 1967). The nebula is heavily embedded and contains a dense group of young stellar objects, some of which appear to have masses of  $\gtrsim 10 M_{\odot}$ , making it the nearest site of massive star formation ( $\sim 400$  pc, Menten et al. 2007; Kim et al. 2008; Kounkel et al. 2017). For one of these massive stars, the Becklin-Neugebauer (BN) object (Becklin & Neugebauer 1967), multi-epoch radio observations have revealed an unusually high proper motion (Plambeck et al. 1995). Members of Orion exhibit a dispersion of  $\sim 1$  mas yr<sup>-1</sup> in their proper motions (van Altena et al. 1988; Dzib et al.

2017), whereas BN has a proper motion of 13.5 mas yr<sup>-1</sup> (26 km s<sup>-1</sup>) relative to the cluster (Rodríguez et al. 2017).

Runaway young stars may arise from dynamical interactions within multiple systems or small stellar groups (Poveda et al. 1967). Because its proper motion is pointed away from the Trapezium stars, it has been proposed that BN was ejected 4000 years ago from a multiple system containing the most massive member of the Trapezium,  $\theta^1$  Ori C (Plambeck et al. 1995; Tan 2004), which also helps explain some of the properties of that system (Chatterjee & Tan 2012). The proper motion of BN indicates that it may have passed near radio source I (Garay et al. 1987; Churchwell et al. 1987) in the KL Nebula ~500 years ago. Tan (2004) suggested that following its ejection from the Trapezium, BN passed close enough to source I to trigger the explosive outflow that emanates from the cloud core in the KL nebula (Allen & Burton 1993). Kinematic studies of the outflow have found that it did originate in the vicinity of source I near that time period (Zapata et al. 2009; Bally et al. 2011). Alternatively, Bally & Zinnecker (2005) and Rodríguez et al. (2005) proposed that BN, source I, and at least one additional star were members of a multiple system, and the latter two stars formed a tight binary or merged, which resulted in the ejection of BN and the generation of the outflow. That scenario has been supported by the measurement of source I's proper motion, which is in roughly the opposite direction of BN's motion (Rodríguez et al. 2005; Goddi et al. 2011). Based on radio measurements of its proper motion, source n from Lonsdale et al. (1982) also may have originated from a multiple system with source I and BN (Gómez et al. 2005, 2008; Rodríguez et al. 2017), although its motion is more difficult to reliably

<sup>1</sup> Based on observations made with the NASA/ESA *Hubble Space Telescope* and the NASA Infrared Telescope Facility.

<sup>2</sup> Department of Astronomy and Astrophysics, The Pennsylvania State University, University Park, PA 16802, USA; kluhman@astro.psu.edu

<sup>3</sup> Center for Exoplanets and Habitable Worlds, The Pennsylvania State University, University Park, PA 16802, USA

<sup>4</sup> Space Telescope Science Institute, 3700 San Martin Drive Baltimore, MD 21218, USA

<sup>5</sup> Johns Hopkins University, Center for Astrophysical Sciences 3400 North Charles Street, Baltimore, MD 21218, USA

<sup>6</sup> Department of Astronomy, University of Florida, Gainesville, FL 32611, USA

<sup>7</sup> Department of Physics, University of Florida, Gainesville, FL 32611, USA

<sup>8</sup> Gemini Observatory, Casilla 603, La Serena, Chile

<sup>9</sup> Dipartimento di Fisica, Università degli Studi di Milano, via Celoria 16, I-20133 Milano, Italy

<sup>10</sup> Scientific Support Office, Directorate of Science, European Space Research and Technology Centre, Keplerlaan 1, 2201 AZ, Noordwijk, The Netherlands

<sup>11</sup> Johns Hopkins University, Department of Physics and Astronomy, 3400 North Charles Street, Baltimore, MD 21218, USA

measure because of its complex and evolving morphology at radio wavelengths (Goddi et al. 2011).

Previous studies have generally favored the KL Nebula rather than the Trapezium as the ejection site for BN (Bally & Zinnecker 2005; Gómez et al. 2008; Goddi et al. 2011). For instance, BN appears to be younger than the Trapezium stars based on its circumstellar material and its ejection from the Trapezium and subsequent close encounter with source I would not account for the large motions of I and n. Nevertheless, some doubts persist regarding this scenario in which BN was ejected from a multiple system with source I (Goddi et al. 2011; Plambeck & Wright 2017). It is challenging to explain the presence of the circumstellar disks around BN and sources I and n if they experienced interactions that were sufficiently close to produce the rapid ejection of BN. In addition, the mass of source I derived by combining an estimate of BN’s mass with conservation of momentum ( $\sim 20 M_{\odot}$ ) is higher than the dynamical mass measured from its circumstellar material ( $\sim 7 M_{\odot}$ , Matthews et al. 2010; Hirota et al. 2014; Plambeck & Wright 2017).

The proper motions of BN, source I, and other stars embedded in the KL Nebula have been previously measured with multi-epoch radio observations. However, many young stars in the nebula are not detected in radio surveys, and instead appear only in IR imaging. To search for large motions among those stars, we have used high-resolution near-IR images that were obtained with the *Hubble Space Telescope* (*HST*) in 1998 and 2015. In this Letter, we report the discovery of a high proper motion for source x from Lonsdale et al. (1982). Based on its motion, source x likely originated from the same multiple system that produced BN and source I. Meanwhile, we find that the proper motion of source n is inconsistent with participation in that event.

## 2. ASTROMETRY IN THE KLEINMANN-LOW NEBULA

To search for high proper motion stars in the KL Nebula that are not detected by radio surveys, we have used images spanning 17 years that were obtained with the Near-Infrared Camera and Multi-Object Spectrometer (NICMOS) and the Wide Field Camera 3 (WFC3, Kimble et al. 2008) on board *HST*. On 1998 January 12 and 16 (UT), camera 3 of NICMOS collected images of the KL Nebula in the filters F110W, F160W, F164N, F166N, F190N, F212N, and F215N (Schultz et al. 1999; Luhman et al. 2000). On 2015 March 13 (UT), WFC3 observed a much larger portion of the Orion Nebula Cluster, including the entirety of the KL Nebula, in the F130N and F139M filters through Treasury program 13826 (M. Robberto, in preparation). The raw images from NICMOS and WFC3 had plate scales of approximately  $0.2'' \text{ pixel}^{-1}$  and  $0.13'' \text{ pixel}^{-1}$ , respectively.

Pixel coordinates for point sources in each of the NICMOS and WFC3 images were measured with the task *starfind* in IRAF. We used astrometry from the near-IR imaging survey of Meingast et al. (2016) for stars in our F130N and F139M WFC3 images to derive offsets in right ascension, declination, and rotation that would align the World Coordinate System (WCS) of the WFC3 images to the astrometric system utilized by Meingast et al. (2016), which was that of the Two Micron All-Sky Survey (Skrutskie et al. 2006). We mea-

sured the WCS of each NICMOS image using astrometry of stars derived from those updated WFC3 images.

For each of the two cameras, we computed the average coordinates of each star from among the filters in which it was detected, excluding data in the corners of the NICMOS images because of the greater uncertainty in the distortion correction. For each star detected by WFC3, we then identified the closest matching star in the catalog of sources from NICMOS. Proper motions were computed with the matched WFC3 and NICMOS coordinates. We estimated the errors in these motions from the standard deviations of the differences in right ascension and declination between the two epochs. These estimates are upper limits for the errors since the velocity dispersion among the stars ( $\sim 1 \text{ mas yr}^{-1}$ , van Altena et al. 1988; Dzib et al. 2017) also contributes to the dispersion in our proper motion measurements.

Among the stars in the vicinity of the KL Nebula, source x from Lonsdale et al. (1982) exhibits the largest motion. Its total proper motion is  $29 \text{ mas yr}^{-1}$ , which corresponds to a velocity of  $55 \text{ km s}^{-1}$  at the distance of Orion. Foreground field stars often have large proper motions, but source x cannot be a foreground star given the high extinction indicated by its red colors (Section 3). Its IR excess emission and spectral features provide additional evidence of youth and membership in Orion (Sections 3 and 4). In Table 1, we list the position of source x in the WFC3 data and its proper motion in right ascension and declination.

BN has the second largest proper motion among stars in the KL Nebula that were detected by WFC3 and NICMOS. We measure a proper motion of  $(\mu_{\alpha}, \mu_{\delta}) = (-6.9 \pm 1.4, +10.3 \pm 1.4 \text{ mas yr}^{-1})$  for BN in the rest frame of Orion, which is consistent with the more accurate measurement at radio wavelengths from Rodríguez et al. (2017). We did not find any additional stars in the KL Nebula with relative proper motions larger than  $2\sigma$  ( $\gtrsim 3 \text{ mas yr}^{-1}$ ).

As discussed in Section 1, some previous studies have reported a fairly large proper motion for source n ( $0 \pm 0.9, -7.8 \pm 0.6 \text{ mas yr}^{-1}$ , Rodríguez et al. 2017). However, we derive a smaller value of  $-1.8 \pm 1.4, -2.5 \pm 1.4 \text{ mas yr}^{-1}$ , which agrees better with the motion of  $+1.6 \pm 1.6, +3.4 \pm 1.6 \text{ mas yr}^{-1}$  measured from millimeter data by Goddi et al. (2011). In centimeter continuum images, source n exhibited two components separated by  $\sim 0''.35$  in early epochs (Gómez et al. 2005) and appeared as a single elongated object in later data (Gómez et al. 2008; Rodríguez et al. 2017). It is unclear which, if any, of the flux peaks in those images correspond to the star, which makes it difficult to reliably measure the star’s motion with those data. Rodríguez et al. (2017) refer to source n as a double star based on the radio morphology, but it is a single point source in the *HST* images.

In Figure 1, we show the NICMOS/F160W and WFC3/F139M images for a  $30'' \times 30''$  field encompassing BN and sources I, n, and x. Source I was not detected in these data (or any previous IR images).

## 3. PHOTOMETRY OF SOURCE X

Since its initial detection at  $1.6$  and  $2.2 \mu\text{m}$  by Lonsdale et al. (1982), source x has been imaged in X-rays (Getman et al. 2005) and in bands from  $1.6$ – $11.7 \mu\text{m}$  (Hillenbrand & Carpenter 2000; Luhman et al.

2000; Lada et al. 2000, 2004; Muench et al. 2002; Robberto et al. 2005, 2010; Smith et al. 2005; Meingast et al. 2016). It has exhibited variations of  $\sim 1$  mag among the multiple measurements that are available in the  $H$  and  $K$  bands. As a result, we have adopted the median of the available  $H - K$  and  $H - K_s$  colors in which the bands were measured near the same time, and we have adopted the median of the available  $K$  and  $K_s$  data. In Table 1, we have compiled those median values and the (single) measurements of  $m_{160}$ ,  $K - L$ ,  $N$ , and  $F_{11.7}$ . Source x was not detected in the F110W image from NICMOS. We note that Favre et al. (2011) detected methyl formate emission at  $1''.9$  from source x. Two other stars also appear within  $3\text{--}4''$  of that emission peak, so it is unclear whether it is associated with source x.

We have measured aperture photometry for source x in the WFC3 images using an aperture radius of two pixels and radii of two and five pixels for the inner and outer boundaries of the sky annulus, respectively. We estimated aperture corrections of 0.166 (F130N) and 0.176 (F139M) between those apertures and radii of  $0''.4$  using bright stars in the WFC3 images. We applied those corrections and the zero-point Vega magnitudes of 21.8258 (F130N) and 23.2093 (F139M) for  $0''.4$  apertures<sup>12</sup> to the photometry of source x. The resulting measurements of  $m_{130}$  and  $m_{139}$  are included in Table 1.

To compare the evolutionary stage of source x to those of BN and source n, we have plotted their near-IR spectral energy distributions (SEDs) in Figure 2. When using bands that are measured near the same time, the colors of source x are similar to or slightly bluer than those of BN and source n, indicating that source x resembles the latter stars in having high extinction and IR excess emission from circumstellar material. For instance, Lada et al. (2000) classified source x as a candidate protostar based on its red  $K - L$  color. However, source x is much bluer than BN and source n between the WFC3 filters and bands at longer wavelengths, as illustrated in Figure 2, which indicates that source x probably brightened by a few magnitudes prior to the WFC3 observations.

#### 4. SPECTROSCOPY OF SOURCE X

Since spectroscopy has not been previously reported for source x, we observed it with the near-IR spectrograph SpeX (Rayner et al. 2003) at the NASA Infrared Telescope Facility (IRTF) on the night of 2017 January 14. The instrument was operated in the SXD mode with the  $0''.8$  slit, which produced data with a resolution of  $R \sim 800$  and a wavelength coverage of  $0.8\text{--}2.5 \mu\text{m}$ . We collected ten 1 min exposures in an ABBA pattern along the slit. To facilitate removal of nebular line emission at the location of source x, we selected A/B positions on the slit that were fairly close to each other ( $3''$ ) and a position angle for the slit ( $30^\circ$ ) that minimized contamination from extended  $\text{H}_2$  emission (Stolovy et al. 1998; Schultz et al. 1999).

The data for source x were reduced with the Spextool package (Cushing et al. 2004) and corrected for telluric absorption in the manner described by Vacca et al. (2003). The spectral images in the A and B slit positions were subtracted from each other to remove sky

emission. Based on the spectra at positions adjacent to source x along the slit, the extended hydrogen and helium emission from the Orion Nebula was successfully removed, and the remaining emission in the spectrum of source x should arise from the star. However, because the  $\text{H}_2$  emission across the KL Nebula varies on small angular scales, our method of sky subtraction produced erroneous negative residuals in the spectrum of source x at the wavelengths of  $\text{H}_2$  lines. Therefore, we have ignored the data at those wavelengths.

The reduced spectrum of source x from  $1.4\text{--}2.4 \mu\text{m}$  is shown in Figure 3. Little flux was detected at shorter wavelengths. In addition to the hydrogen and helium emission lines mentioned earlier, the spectrum exhibits several absorption features from metals and CO. Given the presence of IR excess emission in its SED, these features may be diluted by continuum emission from circumstellar dust. To estimate the spectral type in a way that is independent of such veiling, we have compared the relative strengths of Na I, Ca I, and Mg I at  $2.2\text{--}2.3 \mu\text{m}$  to those measured from SpeX data for field dwarfs (Rayner et al. 2009) and diskless young stars (M. McClure, private communication). We arrive at a spectral type of early K for source x. Its spectrum contains continuum veiling according to both samples of standard stars, but the young stars have stronger atomic lines than the dwarfs, so they imply greater veiling. To illustrate one of the better fits, we have included in Figure 3 a comparison of source x and the young star LkCa 19 (K2, Herczeg & Hillenbrand 2014). The latter has been artificially veiled to match the strengths of Na I, Ca I, and Mg I in source x ( $F_{\text{excess}}/F_* = 0.6$ ). The ratio of the CO bandhead to the atomic lines is higher in source x than in the standards, which indicates a lower surface gravity. The spectral slope of source x indicates an extinction of  $A_V \sim 30$  based on comparison to the best-fitting veiled standards.

#### 5. KINEMATICS OF BN AND SOURCES I AND X

In Figure 4, we plot the positions and proper motion vectors of BN and sources I and x. We have excluded source n since its proper motion constraints from the *HST* images and the millimeter data from Goddi et al. (2011) are significantly smaller than the other measurements that had suggested an origin at the same location as BN and source I (Gómez et al. 2005, 2008; Rodríguez et al. 2017). Based on their relative proper motions, BN and source I experienced their closest approach in the year  $1475 \pm 6$  with a projected separation of  $\lesssim 40$  AU ( $1 \sigma$ , Rodríguez et al. 2017). We have included in Figure 4 the  $1 \sigma$  range of allowed paths for each star back to that year. The estimated location of source x in 1475 agrees with the initial position for the other two stars, which indicates that it was ejected in the same event as those stars. Source x provides strong evidence that such an event did occur and that BN originated in the KL Nebula rather than the Trapezium.

If BN and sources I and x were ejected from a multiple system, they should exhibit little net momentum in the rest frame of Orion. A radial velocity measurement is not available for source x, but we can estimate the net momentum in the plane of the sky with the proper motions. We adopt  $10 M_\odot$  for BN based on its luminosity and ionization rate (Rodríguez et al. 2005) and

<sup>12</sup> [http://www.stsci.edu/hst/wfc3/phot\\_zp\\_lbn](http://www.stsci.edu/hst/wfc3/phot_zp_lbn)

$7 M_{\odot}$  for source I based on the kinematics of its circumstellar material (Matthews et al. 2010; Hirota et al. 2014; Plambeck & Wright 2017). We derive a luminosity of  $\sim 20 L_{\odot}$  for source x using its  $H$ -band magnitude, a bolometric correction for an early K star, and the extinction from our spectrum. By combining that luminosity and the temperature corresponding to an early K star ( $\sim 5000$  K, Schmidt-Kaler 1982) with theoretical evolutionary models (Palla & Stahler 1999), we estimate a mass of  $2.5\text{--}3 M_{\odot}$  for source x. Using these adopted masses and the proper motions, the three stars exhibit a momentum equivalent to a velocity of  $\sim 1.4 \text{ km s}^{-1}$  for the original system in the rest frame of Orion, which is comparable to the velocity dispersion of the cluster. By accounting for the kinematics of source x, we have resolved the previous discrepancy between the dynamical mass of  $7 M_{\odot}$  for source I and the mass of  $\sim 20 M_{\odot}$  implied by conservation of momentum with BN alone (Gómez et al. 2008; Goddi et al. 2011).

Some aspects of the interaction that ejected BN and sources I and x remain unclear, such as how these stars were able to retain or reform their circumstellar disks

(Goddi et al. 2011; Plambeck & Wright 2017) and the source of their current kinetic energy. As discussed in Section 1, the latter has been previously attributed to the gravitational potential energy released by a pair of stars forming a tight binary or merging, likely in what is now source I. The energy produced by the merger of stars with a total mass of source I (e.g., 1 and  $6 M_{\odot}$ ) is an order of magnitude greater than the kinetic energy of the three stars, so that remains a plausible explanation.

This work was supported by grant AST-1208239 from the NSF and grant GO-13826 from the Space Telescope Science Institute. The NASA/ESA *HST* is operated by the Space Telescope Science Institute and the Association of Universities for Research in Astronomy, Inc., under NASA contract NAS 5-26555. The IRTF is operated by the University of Hawaii under contract NNN14CK55B with NASA. The Center for Exoplanets and Habitable Worlds is supported by the Pennsylvania State University, the Eberly College of Science, and the Pennsylvania Space Grant Consortium.

#### REFERENCES

- Allen, D. A., & Burton, M. G. 1993, *Nature*, 363, 54  
 Bally, J., Cunningham, N. J., Moeckel, N., et al. 2011, *ApJ*, 727, 113  
 Bally, J., & Zinnecker, H. 2005, *AJ*, 129, 2281  
 Becklin, E. E., & Neugebauer, G. 1967, *ApJ*, 147, 799  
 Chatterjee, S., & Tan, J. C. 2012, *ApJ*, 754, 152  
 Churchwell, E., Felli, M., Wood, D. O. S., & Massi, M. 1987, *ApJ*, 321, 516  
 Cushing, M. C., Vacca, W. D., & Rayner, J. T. 2004, *PASP*, 116, 362  
 Dzib, S. A., Loinard, L., Rodríguez, L. F., et al. 2017, *ApJ*, 834, 139  
 Favre, C., Despois, D., Brouillet, N., et al. 2011, *A&A*, 532, A32  
 Garay, G., Moran, J. M., & Reid, M. J. 1987, *ApJ*, 314, 535  
 Getman, K. V., Flaccomio, E., Broos, P. B., et al. 2005, *ApJS*, 160, 319  
 Goddi, C., Humphreys, E. M. L., Greenhill, L. J., Chandler, C. J., & Matthews, L. D. 2011, *ApJ*, 728, 15  
 Gómez, L., Rodríguez, L. F., Loindard, L., et al. 2005, *ApJ*, 635, 1166  
 Gómez, L., Rodríguez, L. F., Loindard, L., et al. 2008, *ApJ*, 685, 333  
 Herczeg, G. J., & Hillenbrand, L. A. 2014, *ApJ*, 786, 97  
 Hillenbrand, L. A., & Carpenter, J. M. 2000, *ApJ*, 540, 236  
 Hirota, T., Kim, M. K., Kurono, Y., & Honma, M. 2014, *ApJ*, 782, L28  
 Kim, M. K., Hirota, T., Honma, M., et al. 2008, *PASJ*, 60, 991  
 Kimble, R. A., MacKenty, J. W., O’Connell, R. W., & Townsend, J. A. 2008, *Proc. SPIE*, 7010, 43  
 Kleinmann, D. E., & Low, F. J. 1967, *ApJ*, 149, L1  
 Kounkel, M., Hartmann, L., Loinard, L., et al. 2017, *ApJ*, 834, 142  
 Lada, C. J., Muench, A. A., Haisch, K. E., et al. 2000, *AJ*, 120, 3162  
 Lada, C. J., Muench, A. A., Lada, E. A., & Alves, J. F. 2004, *AJ*, 128, 1254  
 Lonsdale, C. J., Becklin, E. E., Lee, T. J., & Stewart, J. M. 1982, *AJ*, 87, 1819  
 Luhman, K. L., Rieke, G. H., Young, E. T., et al. 2000, *ApJ*, 540, 1016  
 Matthews, L. D., Greenhill, L. J., Goddi, C., et al. 2010, *ApJ*, 708, 80  
 Meingast, S., Alves, J., Mardones, D., et al. 2016, *A&A*, 587, A153  
 Menten, K. M., Reid, M. J., Forbrich, J., & Brunthaler, A. 2007, *A&A*, 474, 515  
 Muench, A. A., Lada, E. A., Lada, C. J., & Alves, J. 2002, *ApJ*, 573, 366  
 Palla, F., & Stahler, S. W. 1999, *ApJ*, 525, 772  
 Plambeck, R. L., & Wright, M. C. H. 2017, *ApJ*, 833, 219  
 Plambeck, R. L., Wright, M. C. H., Mundy, L. G., & Looney, L. W. 1995, *ApJ*, 455, L189  
 Poveda, A., Ruiz, J., & Allen, C. 1967, *Bol. Obs. Tonantzintla Tacubaya*, 4, 86  
 Rayner, J. T., Cushing, M. C., & Vacca, W. D. 2009, *ApJS*, 185, 289  
 Rayner, J. T., Toomey, D. W., Onaka, P. M., et al. 2003, *PASP*, 115, 362  
 Robberto, M., Beckwith, S. V. W., Panagia, N., et al. 2005, *AJ*, 129, 1534  
 Robberto, M., Soderblom, D. R., Scandariato, G., et al. 2010, *AJ*, 139, 950  
 Rodríguez, L. F., Dzib, S. A., Loinard, L., et al. 2017, *ApJ*, 834, 140  
 Rodríguez, L. F., Poveda, A., Lizano, S., & Allen, C. 2005, *ApJ*, 627, L65  
 Schaller, G., Schaerer, D., Meynet, G., & Maeder, A. 1992, *A&AS*, 96, 269  
 Schmidt-Kaler, T. 1982, in *Landolt-Bornstein, Group VI, Vol. 2*, ed. K.-H. Hellwege (Berlin: Springer), 454  
 Schultz, A. S. B., Colgan, S. W. J., Erickson, E. F., et al. 1998, *ApJ*, 511, 282  
 Simon, M., Close, L. M., & Beck, T. L. 1999, *AJ*, 117, 1375  
 Skrutskie, M., Cutri, R. M., Stiening, R., et al. 2006, *AJ*, 131, 1163  
 Smith, N., Bally, J., Shuping, R. Y., Morris, M., & Kassisi, M. 2005, *AJ*, 130, 1763  
 Stolovy, S. R., Burton, M. G., Erickson, E. F., et al. 1998, *ApJ*, 492, L151  
 Tan, J. C. 2004, *ApJ*, 607, L47  
 Vacca, W. D., Cushing, M. C., & Rayner, J. T., 2003, *PASP*, 115, 389  
 van Altena, W. F., Lee, J. T., Lee, J.-F., Lu, P. K., & Upgren, A. R. 1988, *AJ*, 95, 1744  
 Zapata, L. A., Schmid-Burgk, J., Ho, P. T. P., Rodríguez, L. F., & Menten, K. M. 2009, *ApJ*, 704, L45

TABLE 1  
 ASTROMETRY AND PHOTOMETRY OF SOURCE X

Parameter	Value	Reference
$\alpha$ (J2000, epoch 2015.20)	$5^{\text{h}}35^{\text{m}}15.222^{\text{s}}$	1
$\delta$ (J2000, epoch 2015.20)	$-5^{\circ}22'36.96''$	1
$\mu_{\alpha} \cos \delta^{\text{a}}$	$+23.3 \pm 1.4 \text{ mas yr}^{-1}$	1
$\mu_{\delta}^{\text{a}}$	$-17.4 \pm 1.4 \text{ mas yr}^{-1}$	1
$m_{130}$	$15.93 \pm 0.02 \text{ mag}$	1
$m_{139}$	$15.01 \pm 0.02 \text{ mag}$	1
$m_{160}$	$14.38 \pm 0.02 \text{ mag}$	2
$H - K$ and $H - K_s$ (median)	2.58 mag	3,4,5
$K$ and $K_s$ (median)	11.04 mag	3,4,5,6
$K - L$	$2.76 \pm 0.06 \text{ mag}$	4,7
$N$	$6.59 \pm 0.1 \text{ mag}$	8
$F_{\nu}(11.7\mu\text{m})$	0.16 Jy	9

REFERENCES. — (1) this work; (2) Luhman et al. (2000); (3) Hillenbrand & Carpenter (2000); (4) Muench et al. (2002); (5) Robberto et al. (2010); (6) Simon et al. (1999); (7) Lada et al. (2000); (8) Robberto et al. (2005); (9) Smith et al. (2005).

<sup>a</sup> Proper motion in the rest frame of Orion.

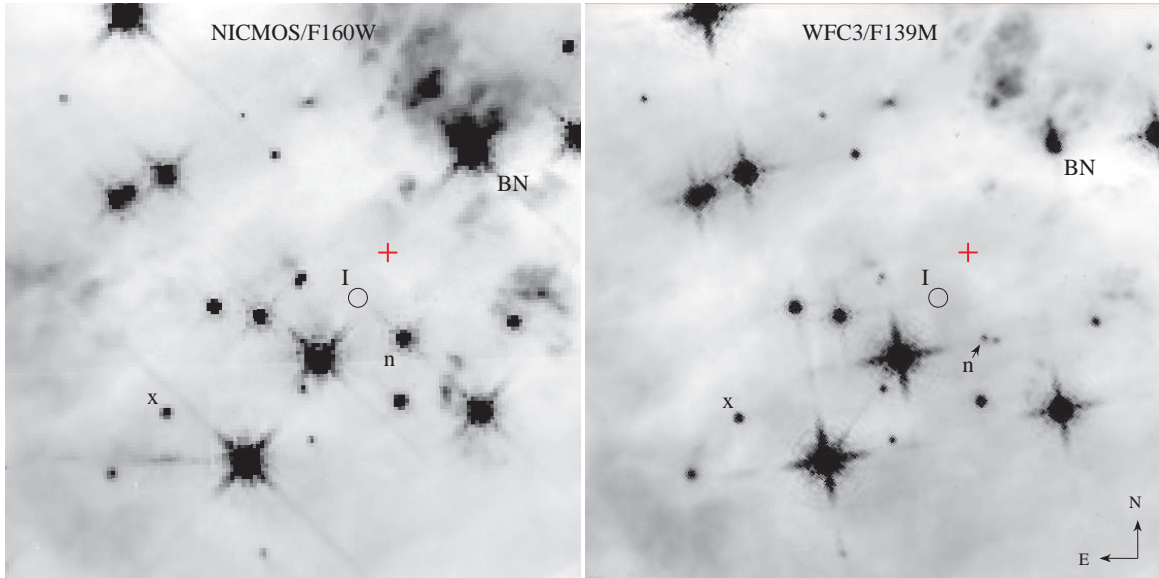


FIG. 1.— Near-IR images of a portion of the KL Nebula from NICMOS in 1998 and WFC3 in 2015. BN and sources n and x are indicated. Source I was not detected in these data; its position at radio wavelengths is circled (Rodríguez et al. 2017). We have marked the initial position of BN and source I in 1475 that was proposed by Rodríguez et al. (2017, cross). The size of each image is  $30'' \times 30''$ .

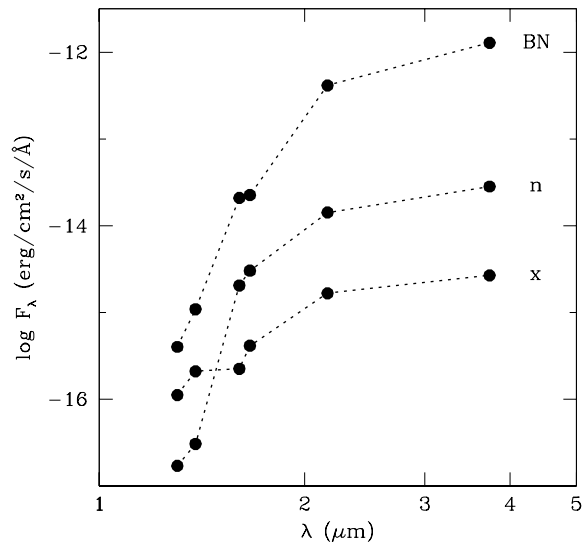


FIG. 2.— Near-IR SEDs for BN and sources n and x (Table 1, 2MASS, Simon et al. 1999; Hillenbrand & Carpenter 2000; Lada et al. 2000; Luhman et al. 2000; Muench et al. 2002; Robberto et al. 2005). The kink in the SED of source x at shorter wavelengths may indicate that it became brighter between the older observations at  $\lambda \geq 1.6 \mu\text{m}$  and the more recent images in F130N and F139M with WFC3.

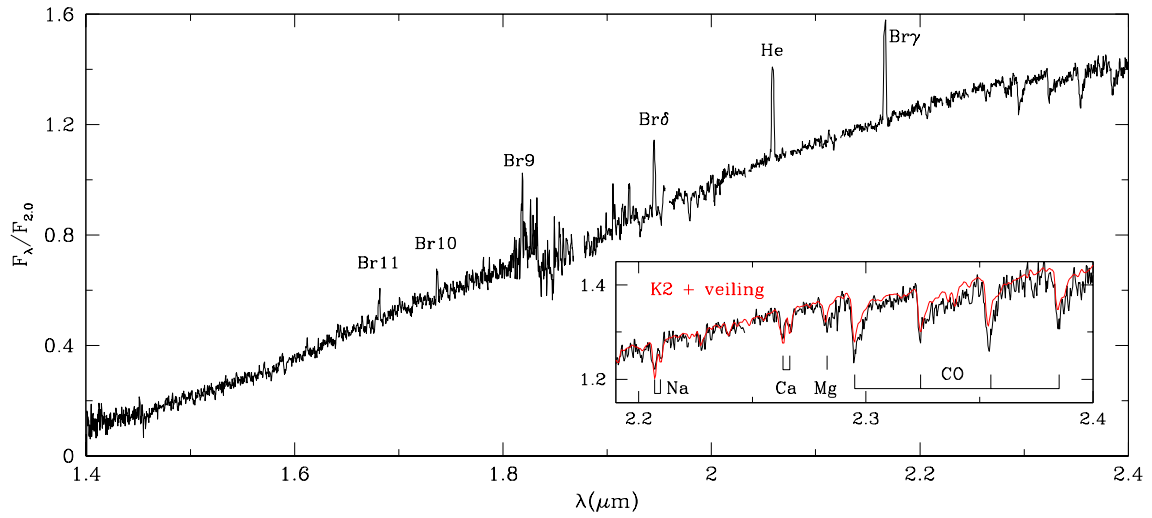


FIG. 3.— Near-IR spectrum of source x ( $R \sim 800$ ). The absorption features are indicative of an early K star with continuum veiling, as illustrated in the inset, where we have applied veiling to a spectrum of LkCa 19 (K2, Herczeg & Hillenbrand 2014) from M. McClure (private communication) to match the strengths of Na, Ca, and Mg in source x. The data used to create this figure are available.

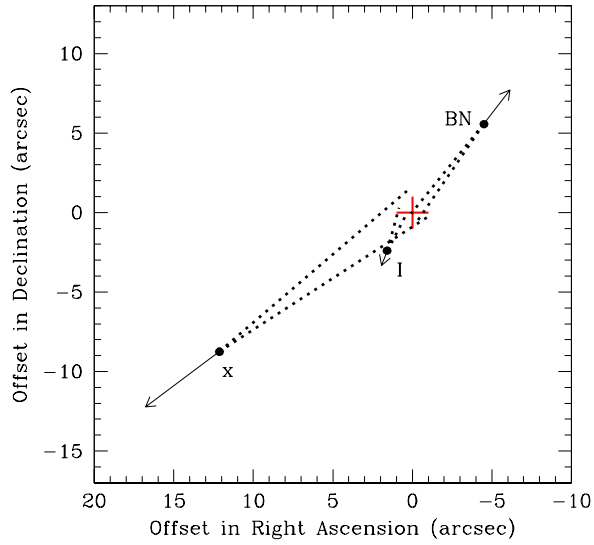


FIG. 4.— Positions of BN and sources I and x (filled circles) for the epoch of the WFC3 images (2015.20) based on astrometry from this work and Rodríguez et al. (2017). The positions are plotted relative to the initial position of BN and I in 1475 that was proposed by Rodríguez et al. (2017, cross). We also show the proper motions in the rest frame of Orion for a period of 200 years (solid lines and arrows) and the range of allowed paths ( $1\sigma$ ) back to 1475 based on those proper motion measurements (dotted lines). The motion of source x is consistent with an origin at the same position and time as the other two stars.